JOURNAL OF VIROLOGY, July 2008, p. 6952–6961 Vol. 82, No. 14
0022-538X/08/$08.00+0 doi:10.1128/JVI.02331-07

Human T-Cell Leukemia Virus Type 1 Tax Attenuates the ATM-Mediated Cellular DNA Damage Response▽

Chandtip Chandhasin,[1]†‡ Razvan I. Ducu,[1]† Elijahu Berkovich,[2] Michael B. Kastan,[2] and Susan J. Marriott[1]*

Department of Molecular Virology and Microbiology, Baylor College of Medicine, One Baylor Plaza, Houston, Texas 77030,[1] and Department of Oncology, St. Jude Children's Research Hospital, Memphis, Tennessee 38105[2]

Received 27 October 2007/Accepted 14 April 2008

Genomic instability, a hallmark of leukemic cells, is associated with malfunctioning cellular responses to DNA damage caused by defective cell cycle checkpoints and/or DNA repair. Adult T-cell leukemia, which can result from infection with human T-cell leukemia virus type 1 (HTLV-1), is associated with extensive genomic instability that has been attributed to the viral oncoprotein Tax. How Tax influences cellular responses to DNA damage to mediate genomic instability, however, remains unclear. Therefore, we investigated the effect of Tax on cellular pathways involved in recognition and repair of DNA double-strand breaks. Premature attenuation of ATM kinase activity and reduced association of MDC1 with repair foci were observed in Tax-expressing cells. Following ionizing radiation-induced S-phase checkpoint activation, Tax-expressing cells progressed more rapidly than non-Tax-expressing cells toward DNA replication. These results demonstrate that Tax expression may allow premature DNA replication in the presence of genomic lesions. Attempts to replicate in the presence of these lesions would result in gradual accumulation of mutations, leading to genome instability and cellular transformation.

Preserving genomic integrity is critical for all living systems. The integrity and survival of a cell depend on the stability of its DNA. Damaged DNA is detected by cellular sensing systems, which activate specific DNA repair pathways. Malfunction of this repair network, collectively known as the DNA damage response, leads to DNA mutations, a subset of which can promote cellular transformation. Double-stranded DNA breaks (DSBs) arise from genotoxic insults and normal physiological processes such as DNA replication (24, 38). The mechanisms by which eukaryotic cells sense DNA breaks remain to be elucidated, but one of the earliest detectable events in DNA damage sensing is the activation of the ataxia telangiectasia mutated (ATM) kinase (45).

ATM is a member of the PI3K-like kinase family and is mutated in ataxia telangiectasia patients (45). Immediately after exposure of cells to DSB-inducing agents such as ionizing radiation (IR) and radiomimetic drugs, changes in chromatin structure activate the intermolecular autophosphorylation of ATM on Ser1981, resulting in the dissociation of inactive ATM dimers into active monomers that allow substrate accessibility to the ATM kinase domain (2). ATM substrates include cellular targets such as NBS1, Chk2, p53, MDC1, histone 2AX (H2AX), and BRCA1, which are key players in the maintenance of genomic integrity (5, 19, 44, 47). Some of these substrates are phosphorylated by ATM in the nucleoplasm, while others are phosphorylated at sites of DNA damage where ATM is recruited via interaction with the Mre11/Rad50/NBS1 (MRN) complex. At sites of DNA breaks within chromatin, the phosphorylation of H2AX and MDC1 by ATM establishes a positive-feedback loop that maintains ATM autophosphorylation and amplifies the DNA damage response (31). Genetic defects in crucial parts of this network lead to a group of human genetic disorders collectively called genomic instability syndromes. These diseases are characterized by degeneration of specific tissues, sensitivity to DNA-damaging agents, chromosomal instability, and a marked predisposition to cancer (38).

Nearly 70% of all cancers demonstrate chromosomal abnormalities, suggesting a close association between genome instability and carcinogenesis. Infection with human T-cell leukemia virus type 1 (HTLV-1), an oncogenic retrovirus, is associated with the development of adult T-cell leukemia, an aggressive clonal malignancy of $CD4^+$ T cells (20). Adult T-cell leukemia develops in 2% to 5% of HTLV-1-infected individuals after a clinical latency of 20 to 40 years, providing a useful model in which to study the multistep process of HTLV-1-mediated leukemogenesis. HTLV-1 encodes a 40-kDa protein, Tax, which is essential for virus replication and is the major viral oncoprotein (21). Tax-mediated transformation is thought to depend on its ability to perturb normal cellular processes such as gene expression, cell cycle checkpoints, and DNA damage repair (32). Generally, Tax interferes with these processes by interacting with cellular proteins and modifying their function. More than 20 cellular proteins interact with Tax, including MEKK1, MAD1, Rb, IκB kinase subunits, NFκB, Chk1, TATA-binding protein, TFIIEE, and $p16^{INK4a}$ (6, 7, 25, 28, 40, 48, 51, 52). Interactions of Tax with these proteins interfere with normal cellular processes and enhance the propensity of a cell to become transformed.

HTLV-1-transformed cells display extensive genome instability, a hallmark of cancer cells that is typically associated with defects in the recognition and/or repair of DNA damage. Here we

* Corresponding author. Mailing address: Department of Molecular Virology and Microbiology, Baylor College of Medicine, One Baylor Plaza, Houston, TX 77030. Phone: (713) 798-4440. Fax: (713) 798-4435. E-mail: susanm@bcm.edu.

† C.C. and R.I.D. contributed equally to the work.

‡ Present address: Department of Investigational Cancer Therapeutics, M.D. Anderson Cancer Center, 1515 Holcombe Blvd. Unit 455, Houston, TX 77030.

▽ Published ahead of print on 23 April 2008.

investigated the effect of Tax on the recognition and repair of DSBs. We found that Tax expression prematurely attenuates ATM activity, due to defects in ATM accumulation around DNA breaks and subsequent disruption of positive-feedback signals that are required to maintain ATM activity. This attenuation resulted in early release of cells from the IR-induced S-phase checkpoint, despite incomplete DNA repair. Attenuation of ATM activity and its diminished damage-induced recruitment to chromatin correlated with reduced recruitment of MDC1 to repair foci. As a consequence, Tax-expressing cells fail to maintain the ATM-mediated DNA damage response, resulting in premature DNA replication in the presence of genomic lesions. Interference with ATM-mediated DNA damage recognition and repair results in attempted replication through these lesions, which can gradually increase the mutation load, leading to genomic instability and cellular transformation.

MATERIALS AND METHODS

Cell culture and treatments. CREF-Neo and CREF-Tax cells were previously described (27) and were maintained in Dulbecco's modified Eagle medium supplemented with 10% fetal bovine serum (FBS). 293 cells were grown in Dulbecco's modified Eagle medium supplemented with 10% FBS and were transfected with Lipofectamine (Invitrogen, Carlsbad, CA) following the manufacturer's instructions. HTLV-1-negative (CEM and Molt4) and HTLV-1-positive (MT4 and Hut102) human T-cell lines were maintained in RPMI media containing 10% FBS. All cells were grown in a humidified atmosphere at 37°C in 5% CO_2. Exponentially growing cells were either subjected to mock treatment or treated with IR at the indicated doses or with 50 uM bleomycin (Sigma-Aldrich, St. Louis, MO). Cells were allowed to recover at 37°C and were harvested at the indicated time points.

Cell lysis and immunoblotting. Cells were lysed in radioimmunoprecipitation assay buffer (50 mM Tris-HCl [pH 7.4], 1% Nonidet P-40 [NP-40], 0.25% sodium deoxycholate, 150 mM NaCl, 1 mM EDTA, 1 mM phenylmethylsulfonyl fluoride, 1 mM Na_3VO_4, 1 mM NaF, protease inhibitor cocktail) on ice for 10 min, followed by centrifugation at 10,000 rpm for 10 min at 4°C. The supernatant was collected, resolved on 4 to 20% sodium dodecyl sulfate-polyacrylamide gel electrophoresis (SDS-PAGE) gradient gels (Invitrogen, Carlsbad, CA), transferred to polyvinylidene difluoride membranes, and subjected to immunoblotting. Anti-Tax antibody Tab170 was obtained from the AIDS Research and Reference Reagent Program, Germantown, MD, and anti-Tax antibody 586 was obtained from John Brady (National Institutes of Health). Mouse anti-ATM antibody (2C1) was purchased from Santa Cruz Biotechnology (Santa Cruz, CA). Mouse anti-ATM (pS1981) was purchased from Rockland Immunochemicals (Gilbertsville, PA). Antibodies against NBS1, NBS1 (pS343), Chk2 (pT68), Mre11, and H2AX (pS139) were purchased from Cell Signaling Technology (Danvers, MA). Horseradish peroxidase-conjugated secondary antibodies were purchased from Sigma-Aldrich (St. Louis, MO).

Radio-resistant DNA synthesis (RDS) assay. The rate of DNA synthesis was measured by the ^{14}C-/^{3}H-thymidine double-labeling method as previously described (50). Briefly, actively growing cells were prelabeled with [^{14}C]thymidine (MP Biochemicals, Inc.) (20 nCi/ml [55.4 mCi/mmol]) for 24 h to normalize for total DNA content. Excess ^{14}C was removed by washing with phosphate-buffered saline, and cells were allowed to rest for 24 h in normal medium. Cells were irradiated at the indicated doses and allowed to recover at 37°C. At the indicated time points, cells were pulse-labeled with [^{3}H]thymidine (MP Biochemicals, Inc.) (2.5 mCi/ml [20 Ci/mmol]) for 15 min, harvested, fixed in 70% methanol, and collected on glass microfiber filters (Whatman GF/C). Dried filters were rinsed sequentially with 70% and 95% methanol and then air dried. The radioactivity of each sample was quantified using a liquid scintillation counter (Beckman LS3801) with windows set to record both ^{14}C and ^{3}H counts per minute. We calculated percent DNA synthesis after exposure to IR as follows: [($^{3}H/^{14}C$ ratio in irradiated cells)/($^{3}H/^{14}C$ ratio in unirradiated cells)] × 100.

CometAssay (single-cell gel electrophoresis). The neutral comet assay was performed using a comet assay kit (CometAssay [silver staining]; R&D Systems, Minneapolis, MN) according to the manufacturer's protocol. Briefly, cells were washed, immobilized in a bed of agarose, and subjected to electrophoresis. Under the influence of an electric field, damaged DNA migrates away from the nucleus, forming a comet-shaped tail, whereas undamaged DNA remains intact in the nucleus. The ratio of the number of cells containing comets to the total number of cells, as well as the average comet tail length, was quantified for 200 cells per sample.

Cellular fractionation. Fractionation of cells was performed as previously described (1). Briefly, 10^7 cells were washed twice with ice-cold phosphate-buffered saline and resuspended for 5 min on ice in 150 μl of fractionation buffer (50 mM HEPES [pH 7.5], 150 mM NaCl, 1 mM EDTA, 10 mM NaF, 1 mM sodium orthovanadate, protease inhibitors) containing 0.2% NP-40. Following centrifugation at 1,000 × *g* for 5 min, the supernatant was collected (fraction I), and pellets were washed with the same buffer. The wash was collected (fraction II), and cells were further extracted for 40 min on ice with 150 μl of fractionation buffer containing 0.5% NP-40. Samples were centrifuged at 16,000 × *g* for 15 min, and supernatants were collected (fraction III). The remaining pellets (fraction IV) were lysed in LDS sample buffer (Invitrogen, Carlsbad, CA), sonicated, and boiled for 10 min. Equal aliquots of each fraction, derived from equivalent cell numbers, were separated on 4% to 20% SDS-PAGE gradient gels (Invitrogen, Carlsbad, CA).

Immunofluorescent staining. Cells were seeded on ethanol-washed coverslips and grown to approximately 50% confluence before exposure to genotoxic conditions. The cells were washed once with PEM buffer {80 mM potassium PIPES [piperazine-*N*,*N*′-bis(2-ethanesulfonic acid); pH 6.8], 5 mM EGTA (pH 7.0), 2 mM $MgCl_2$} and fixed by incubation in 5% formaldehyde diluted in PEM buffer for 30 min at 4°C. To remove excess formaldehyde, cells were washed three times in PEM buffer and permeabilized by incubation in PEM buffer containing 0.5% Triton X-100 for 30 min at room temperature. Immunofluorescent staining was performed by incubating with primary antibody diluted in 5% bovine serum albumin containing Tris-buffered saline–0.1% Tween 20 (TBS-T) for a minimum of 3 h at room temperature. Excess antibody was removed by washing cells three times in TBS-T. Cells were incubated, in the dark, with a fluorophore-conjugated secondary antibody diluted in TBS-T for 40 min at room temperature. Excess antibody was removed by washing the coverslips three times with TBS-T. The cells were stained with DAPI (4′,6-diamidino-2-phenylindole) (Sigma-Aldrich, St. Louis, MO) to visualize the nucleus and mounted on slides by use of SlowFade antifade mounting medium (Molecular Probes, Eugene, OR). Cells were visualized using a Zeiss AxioPlan2 microscope and a CoolSnap HQ charge-coupled device camera. For deconvolved images (see Fig. 6A and 7), an Applied Precision microscope and softWoRx Image Restoration software were utilized.

RESULTS

Tax antagonizes ATM activation and kinase activity. Activation of ATM kinase is one of the first detectable steps in the response to DSBs. To determine whether Tax affects ATM kinase activation in response to DNA damage, HTLV-1-positive and -negative human T cells were exposed to IR and ATM phosphorylation at serine 1981 was assessed at various time points following DNA damage. In HTLV-1-negative T cells (Molt4 and CEM), ATM phosphorylation at serine 1981 was detected by 30 min following DNA damage and remained stable for at least 3 h thereafter (Fig. 1A). In HTLV-1-positive T cells (Hut102 and MT4), phosphorylated ATM was also detected by 30 min post-IR at levels similar to those seen in uninfected cells. However, ATM phosphorylation was significantly reduced at subsequent time points. These results demonstrate that ATM becomes autophosphorylated in the presence of Tax but that this phosphorylation is transient. Similar effects of Tax on the phosphorylation kinetics of ATM and its substrates were observed following DNA damage in rat embryo fibroblasts that stably express Tax (Fig. 1B) and in 293T cells transfected with a Tax expression vector (Fig. 2). These results indicated that transient ATM phosphorylation was due specifically to Tax expression and did not require other viral proteins. Also, transient ATM phosphorylation was not due to cellular changes that rendered constitutive Tax expression permissible, since the same phenotype was observed in cells transiently expressing Tax. Because ATM autophosphorylation re-

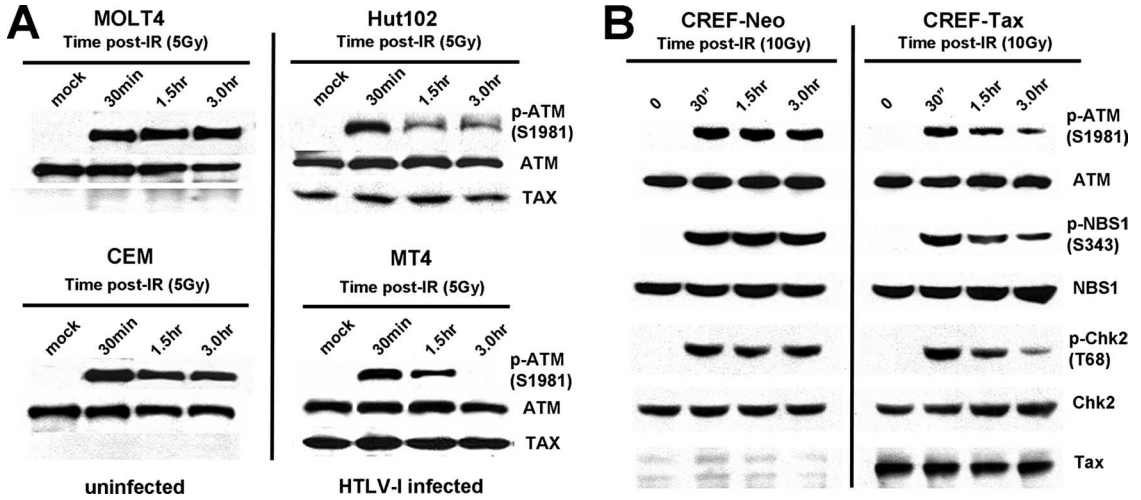

FIG. 1. Tax attenuates ATM autophosphorylation and kinase activity following DNA damage. (A) Western blot analysis of phosphorylated p-ATM (S1981), ATM, and Tax in extracts prepared from uninfected (MOLT4 and CEM) and HTLV-1-infected (Hut102 and MT4) human T cells at the indicated times following exposure to 5 Gy of IR. (B) Western blot analysis of p-ATM (S1981), ATM, p-NBS1 (S343), NBS1, p-Chk2 (T68), Chk2, and Tax in extracts prepared from cloned rat embryonic fibroblasts stably expressing Tax (CREF-Tax) or a neomycin control (CREF-NEO) at the indicated times following exposure to 10 Gy of IR.

sults obtained with Tax-positive and Tax-negative cell lines 30 min after DNA damage were comparable, it appears that Tax did not have a significant effect on ATM activation. However, the reduced ATM phosphorylation observed in Tax-expressing cells at 3 h post-IR suggests that Tax interferes with components of the ATM pathway that maintain ATM activity.

To determine whether the transient phosphorylation of ATM observed in HTLV-1-infected cells affected ATM kinase activity, we examined the phosphorylation status of ATM substrates NBS1 and Chk2 at serine 343 and threonine 68, respectively (10, 17). As was seen with ATM, phosphorylation of NBS1 and Chk2, both of which are direct targets of ATM kinase activity, was induced in Tax-expressing (CREF-Tax) and non-Tax-expressing (CREF-Neo) cells at 30 min post-IR (Fig. 1B). Total NBS1 and Chk2 results remained relatively constant for both cell types before and after damage. Phosphorylation of NBS1 and Chk2 was also attenuated more rapidly in Tax-expressing cells than in non-Tax-expressing cells. Thus, the rapid loss of phosphorylated ATM that is associated with Tax expression correlates with attenuation of ATM kinase activity. These results demonstrate that ATM kinase activity is prematurely attenuated following DNA damage in Tax-expressing cells and that Tax turns off the ATM-mediated DNA damage response.

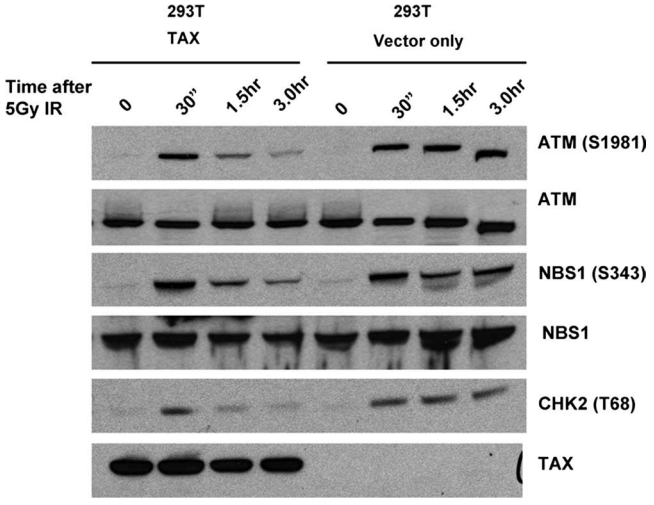

FIG. 2. Attenuation of ATM autophosphorylation and kinase activity following DNA damage in cells transiently expressing Tax. The results of Western blot analysis of phosphorylated p-ATM (S1981), ATM, p-NBS1 (S343), NBS1, p-Chk2 (T68), and Tax in extracts prepared from vector-transfected or Tax-transfected 293T cells at the indicated times following exposure to 5 Gy of IR are shown.

Tax-expressing cells synthesize DNA following ionizing irradiation. Normal cells respond to IR by activating the S-phase checkpoint, thereby transiently blocking DNA replication so that DNA lesions can be repaired. Cells lacking ATM cannot effectively inhibit DNA replication and thus fail to obey the S-phase checkpoint and exhibit RDS (39). Phosphorylation of NBS1 and Chk2, key downstream effectors of the ATM pathway, is required for the S-phase checkpoint (13, 37). Since ATM, NBS1, and Chk2 phosphorylation is prematurely attenuated in Tax-expressing cells, we predicted that Tax expression would lead to defects in the S-phase checkpoint. To test this prediction, CREF-Neo and CREF-Tax cells were exposed to 5 Gy or 10 Gy of IR, and DNA replication was examined 30 min later using an RDS assay. At this time point, similar decreases in DNA replication were observed in both cell lines (Fig. 3A), indicating that the S-phase checkpoint had been successfully established. The reduced DNA replication seen in CREF-Neo and CREF-Tax cells following IR was comparable to levels reported previously for IR-induced downregulation of DNA replication in other cell lines that exhibit a functional S-phase checkpoint (46). Interestingly, time-course analysis of DNA synthesis following IR showed that CREF-Tax cells displayed inhibition of DNA synthesis of shorter duration than CREF-Neo cells (Fig. 3B). By 1 h post-IR, CREF-Tax cells exhibited

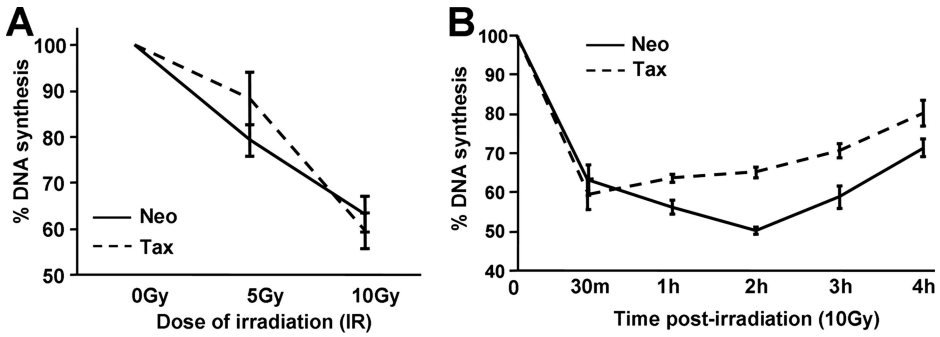

FIG. 3. Tax-expressing cells do not undergo RDS but exhibit a shorter S-phase checkpoint following IR. The integrity of the S-phase checkpoint was analyzed using rat embryonic fibroblast (CREF) cells stably expressing Tax (Tax) or neomycin control (Neo) cells by use of an RDS assay. (A) DNA synthesis in CREF-Neo and CREF-Tax cells was assessed for 30 min after irradiation at the indicated doses. (B) CREF-Neo and CREF-Tax cells were assessed for DNA synthesis at various times after treatment with 10 Gy of IR. This experiment was performed three times. Error bars represent standard deviations of the means.

significantly more DNA synthesis than CREF-Neo cells and this difference was observed through 4 h post-IR. Thus, CREF-Tax cells are released from the S-phase checkpoint to resume DNA replication earlier than control cells. The transient nature of the S-phase checkpoint is likely due to the rapid loss of active, phospho-ATM in Tax-expressing cells. These results suggest that the initial activation of ATM must be followed by sustained ATM activity in order to maintain the S-phase checkpoint. Premature initiation of DNA synthesis following damage would promote the accumulation of DNA mutations and chromosome breakage.

Repair of DSBs is defective in Tax-expressing cells. The inability of Tax-expressing cells to maintain ATM phosphorylation and activity could be due to a defect in the DNA damage response. Alternatively, Tax-expressing cells may not receive as much damage as or may repair DNA damage more efficiently than control cells, thereby causing a valid release of the checkpoint earlier than control cells. To determine which of these possibilities explains the shorter S-phase checkpoint time period that was observed in experiments using Tax-expressing cells, the level of DSBs induced by the radiomimetic drug bleomycin, as well as the kinetics of DNA repair, was determined using a comet assay.

HTLV-1-positive (MT4) and HTLV-1-negative (CEM) T cells were either subjected to mock treatment or treated for 1 h with 50 μM bleomycin. After 1 h of drug exposure, medium containing the drug was removed and replaced with regular medium and the cells were allowed to recover for the indicated times (Fig. 4A). The percentage of cells that displayed a comet tail represented the percentage of cells that contained detectable amounts of DNA damage (Fig. 4B), while the average length of the comet tail represented the amount of DNA damage within the individual cell (Fig. 4C). In the two cell lines, comparable levels of DNA damage were observed following 1 h of bleomycin treatment (Fig. 4B and C, 0 hrs column). In CEM cells, the number and length of bleomycin-induced comet tails were significantly reduced by 24 h. However, a significant amount of broken DNA remained in Tax-expressing MT4 cells up to 24 h after damage (Fig. 4), indicating that MT4 cells were defective in DNA repair. Importantly, Tax expression did not induce significant damage in the absence of bleomycin, since mock-treated MT4 cells did not display comet tails. In addition, Tax did not protect cells from DNA damage, since similar comet tails were observed in cells with and without Tax expression immediately after DNA damage (0 hrs column). Combined with results from the previous experiment, these results suggest that premature inactivation of the S-phase checkpoint in Tax-expressing cells was not due to faster DNA repair. Rather, Tax-expressing cells resumed DNA replication at a time when the cells still contained DNA lesions. Failure to amplify and maintain ATM signaling may have been responsible for the DNA repair defects observed in Tax-expressing cells.

Defective formation of DNA repair foci in Tax-expressing cells following IR. In response to IR, ATM propagates the damage signal by relocating to sites of DNA damage on chromatin and phosphorylating the histone variant H2AX at serine residue 139. Phosphorylated H2AX, referred to as γH2AX, can be detected within minutes after exposure to IR and occurs over large chromatin domains surrounding the DNA break and can be visualized as foci (43). The accumulation of γH2AX is the signal that leads to retention of DNA damage-response factors, including phospho-ATM, at DNA breaks (3, 9, 14), possibly by serving as a docking site for these DNA damage-repair proteins (3). Alternatively, γH2AX may modulate chromatin structure, thereby indirectly facilitating the accumulation of repair proteins (14). γH2AX-mediated retention of repair proteins at the DNA break induces a positive-feedback loop that maintains ATM activation and further amplifies γH2AX (31). If H2AX is not phosphorylated, or proteins are not assembled properly at sites of damage, this feedback loop cannot be maintained and the DNA damage response is not functional (31).

Considering the requirement for H2AX phosphorylation to maintain the ATM-mediated damage response, we examined the effect of Tax on this event. In CREF-Neo cells, H2AX was rapidly phosphorylated, and large discrete foci were observed within 30 min of IR (Fig. 5A, top panels). Time course analysis of H2AX phosphorylation by Western blotting revealed that γH2AX levels continued to increase for up to 3 h after IR in CREF-Neo cells (Fig. 5B, top panel). In contrast, γH2AX foci were much less intense in CREF-Tax cells following IR (Fig. 5A, bottom panels). Examination of γH2AX kinetics in CREF-Tax cells by Western blot analysis showed a very weak γH2AX signal over the time

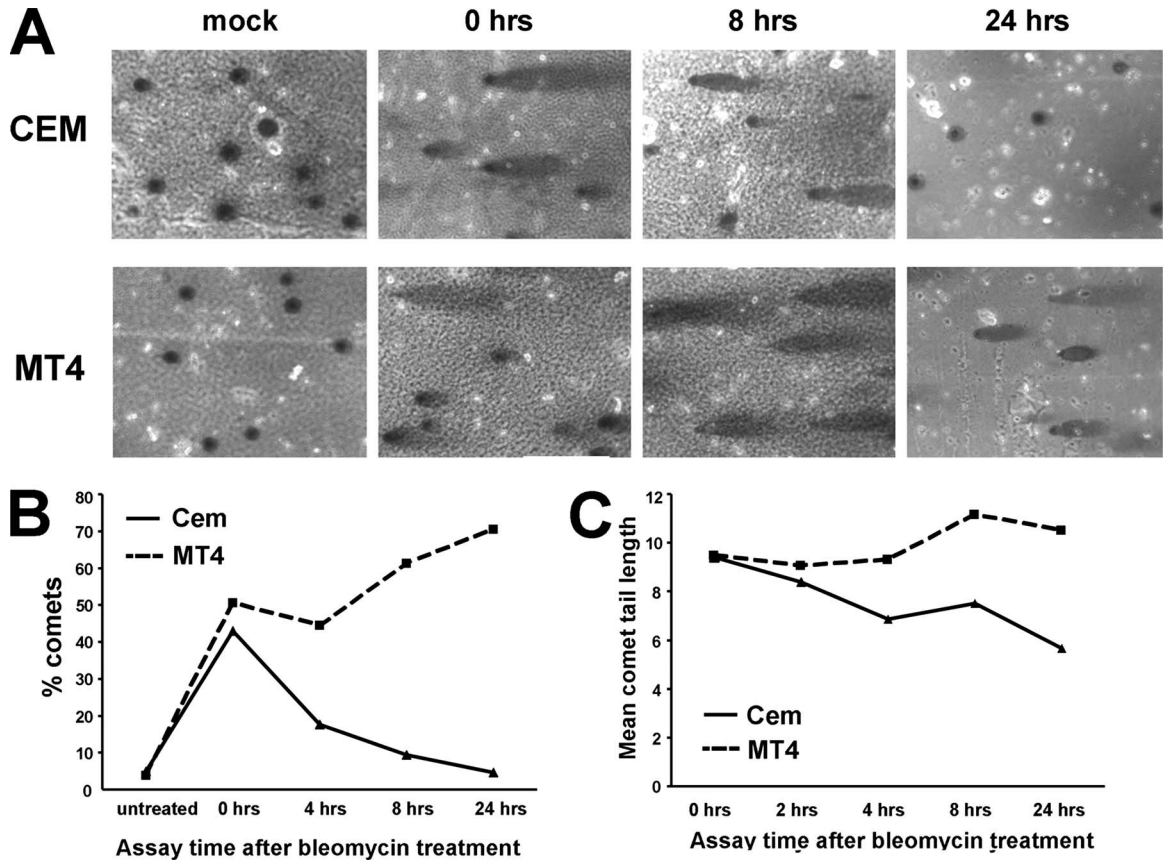

FIG. 4. Repair of DSBs is defective in Tax-expressing cells. (A) Uninfected (CEM) and HTLV-1-infected (MT4) human T cells were treated with 50 uM bleomycin for 1 h, washed twice in regular media, and allowed to recover for the indicated times. Cells were washed and processed for single-cell gel electrophoresis using a comet assay (silver staining) kit. (B and C) The ratios of numbers of cells containing comet tails to total cell numbers (B) and the average comet tail lengths (C) are shown. A total of 200 cells were counted for each slide. This experiment was done three times with similar results. Results of a single representative experiment are shown.

course, with little or no propagation in response to DNA damage (Fig. 5B, bottom panel). HTLV-1-infected T cells (Hut102) also showed less propagation of γH2AX following IR than did HTLV-1-negative T cells (CEM) (Fig. 5C). These results demonstrate a defect in γH2AX amplification in Tax-expressing cells.

Since relocalization and accumulation of ATM at DNA breaks is required for γH2AX phosphorylation and DNA damage signal amplification, these results are consistent with a defect in the accumulation of ATM at sites of DNA damage in Tax-expressing cells. To test this possibility, we performed immunofluorescence staining using anti-phospho-ATM antibody. Activated ATM accumulates near DNA breaks, as demonstrated by the formation of foci detected by use of anti-phospho-S1981 ATM antibody (2). In CREF-Neo cells, p-ATM foci were evident by 30 min following IR and colocalized with γH2AX foci (Fig. 6, left panels), indicating that activated ATM is recruited and retained at sites of DSBs. Although comparable levels of ATM autophosphorylation were observed in CREF-Tax cells after treatment with 10 Gy of IR (Fig. 1B), phospho-ATM did not accumulate into large discrete foci as seen in CREF-Neo cells. Furthermore, γH2AX staining in CREF-Tax cells was very weak and foci were smaller than those observed in CREF-Neo cells (Fig. 6, right panels), despite the presence of DNA damage, as shown by comet assay results. The presence of much smaller and more diffuse ATM foci in Tax-expressing cells indicates that Tax expression disrupted ATM accumulation in the proximity of DNA lesions. By interfering with the accumulation of ATM at DNA breaks, Tax appeared to prevent efficient phosphorylation of H2AX over megabases required to amplify and stabilize repair foci.

Tax alters ATM association with chromatin following DNA damage. To confirm that Tax interferes with the accumulation of ATM at DSBs following DNA damage, we performed a cellular fractionation assay based on successive detergent extractions, a procedure that removes chromatin-associated proteins according to their level of affinity (1). In the absence of DNA damage by bleomycin treatment, the majority of the ATM pool in both CREF-Neo and CREF-Tax cells was released at early extraction steps (fractions I and II), with small amounts of ATM being recovered after longer incubation with detergent (fraction III). No ATM was observed in the most tightly chromatin associated fraction, fraction IV (Fig. 7A, top panel). Treatment of CREF-Neo cells with bleomycin prior to fractionation resulted in an approximately twofold-greater amount of ATM in chromatin-associated fractions III and IV than in the equivalent fractions from untreated cells. Since ATM plays a critical role in detecting DNA damage but is not directly involved in the actual repair process, only a fraction of

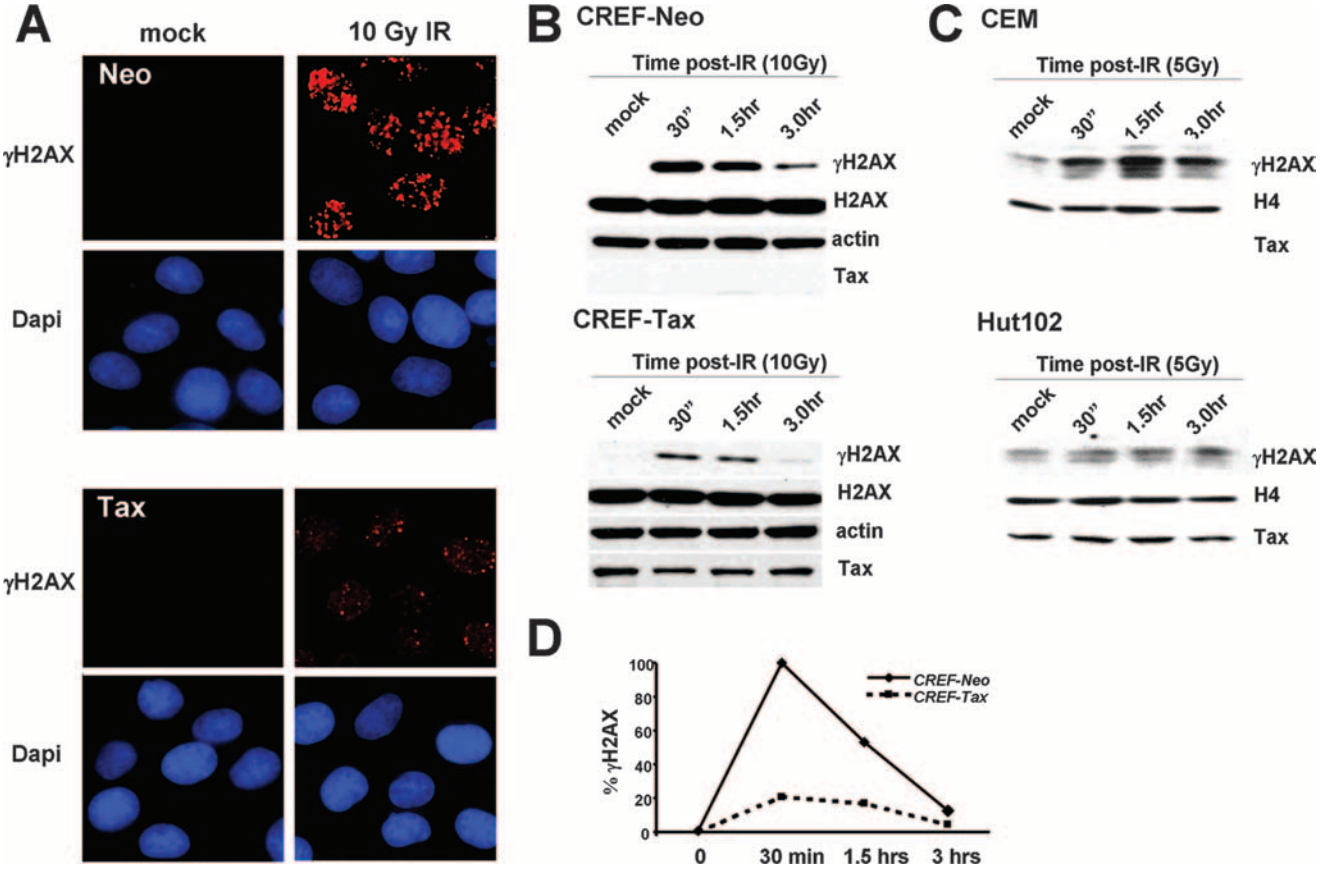

FIG. 5. γH2AX levels are reduced in Tax-expressing cells following DNA damage. (A) Immunofluorescent staining of γH2AX (red) and DAPI staining (blue) in CREF-Neo (Neo) and CREF-Tax (Tax) cells at 30 min after exposure to IR (10 Gy). Images were taken at a magnification of ×63. (B and C) Western blot analysis of γH2AX, total H2AX, actin, H4, and Tax in extracts prepared from CREF-Neo and CREF-Tax (B) or CEM and HuT102 (C) cells at the indicated times following exposure to IR. (D) Densitometric analysis of the data shown in panel B was used to calculate the percentage of γH2AX at each time point using the formula $(\gamma H2AX_A/\text{total } H2AX_A)/(\gamma H2AX_B/\text{total } H2AX_B) \times 100$, where A represents densitometric volumes for each individual time point and B represents densitometric volumes of CREF-Neo cells 30 min after gamma irradiation.

ATM associates with sites of damage (1). Bleomycin treatment of CREF-Tax cells did not significantly alter the amount of ATM in fractions III and IV, suggesting either that ATM does not accumulate on chromatin after induction of DNA damage or that ATM is more sensitive to detergent extraction in Tax-expressing cells. Since the accumulation of phospho-ATM was not observed by immunofluorescence (Fig. 6), we favor a scenario in which Tax interferes with the accumulation of ATM on chromatin following induction of DNA damage.

The cellular fractions analyzed above were also examined by immunoblot analysis for the presence of other proteins involved in DSB repair. Similar levels of Mre11, a nuclease that binds free DNA ends during DNA replication and recombination, were observed in all fractions of mock-treated CREF-Neo and CREF-Tax cells (Fig. 7A). After bleomycin treatment, the amount of Mre11 in fraction IV increased approximately twofold in both cell lines, as is consistent with ATM-independent relocalization of Mre11 to DSBs following DNA damage (33, 34). γH2AX was observed in chromatin-enriched fraction IV after bleomycin treatment, and H2AX levels were 3.5-fold higher in CREF-Neo cells than in CREF-Tax cells. Interestingly, Tax was recovered in all fractions of cells independently of the presence of DNA damage, which is consistent with the known subcellular localization of Tax in distinct complexes with differing functions. Histone H4 was used as a marker of a tightly chromatin-associated protein.

Tax disrupts the association of MDC1 with γH2AX. To gain a better mechanistic understanding of how Tax inhibits the ATM-mediated DNA damage signaling pathway, we investigated possible effects of Tax on the recruitment of MDC1 to damage foci. In parallel with ATM autophosphorylation, the induction of DNA breaks causes the binding of MRN complexes to newly formed DNA ends (34, 53). ATM is then recruited to the damaged sites by interacting with the C-terminal domain of Nbs1 (12, 53). This initial activation and recruitment of ATM by the MRN complex has been hypothesized to induce the phosphorylation of H2AX adjacent to the break site (5). Subsequently, MDC1 binds to both Ser139-phosphorylated H2AX and to ATM, through two separate domains (31). In doing so, MDC1 bridges the interaction of ATM and H2AX, facilitating the accumulation of activated ATM near sites of DNA damage and the rapid expansion of H2AX phosphorylation over megabase regions surrounding DSBs (31).

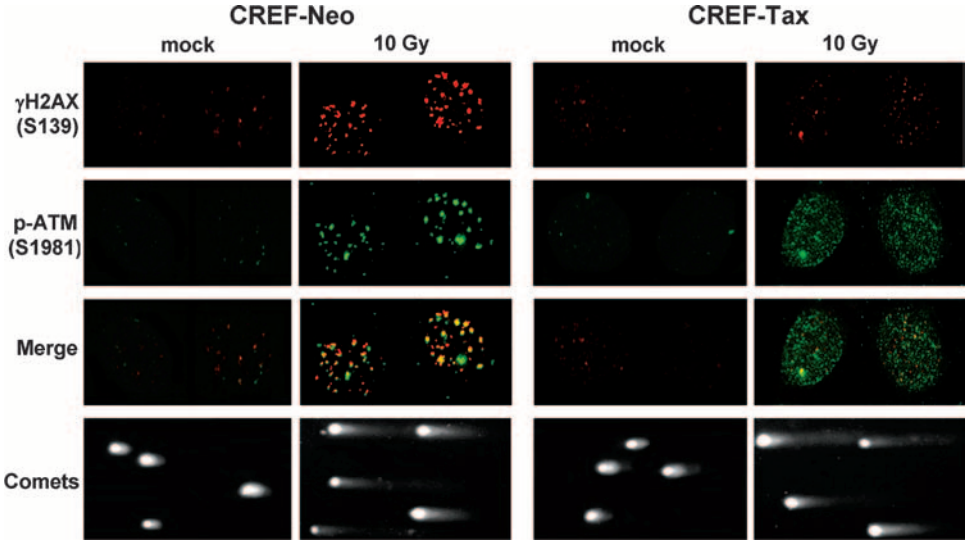

FIG. 6. Tax-expressing cells exhibit defective focus formation following DNA damage. CREF-Neo and CREF-Tax cells were either mock treated or exposed to 10 Gy of IR. After 30 min, cells were collected for DNA damage analysis using a comet assay or were fixed and costained with anti-γH2AX (S139) (red) and anti-p-ATM (S1981) (green) antibodies. A merged image of γH2AX and p-ATM foci is also shown. Deconvolved images were taken at a magnification of ×63 with an Applied Precision microscope and analyzed with softWoRx image restoration software.

To determine whether the initial recruitment of ATM to DNA ends is altered by Tax, the interaction of ATM and Nbs1 was examined by coimmunoprecipitation. We found an association between ATM and Nbs1 after induction of DNA damage, and this binding was not disrupted by the presence of Tax (Fig. 7B). Thus, Tax does not appear to interfere with initial events of the ATM-mediated DNA damage response, including ATM autophosphorylation, its interaction with Nbs1, and the recruitment of Mre11 to chromatin following DNA damage. To determine the integrity of the MDC1-mediated ATM

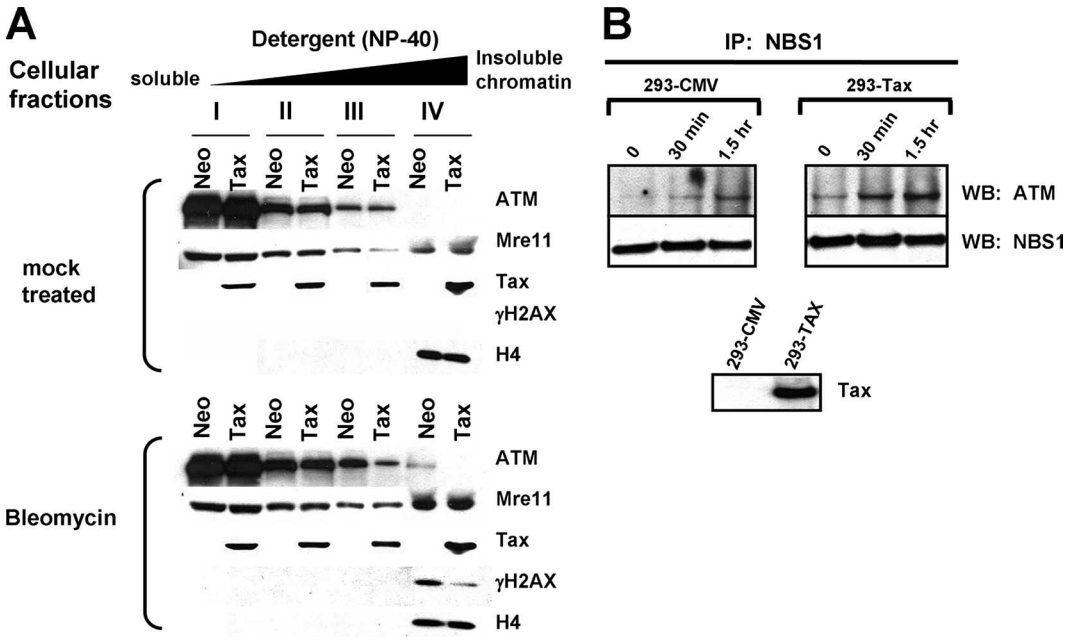

FIG. 7. Tax interferes with the association of ATM with chromatin following DNA damage without disrupting the ATM-Nbs1 interaction. (A) CREF-Neo (Neo) or CREF-Tax (Tax) cells were subjected to mock treatment (top) or treated with 50 μM bleomycin (bottom) for 1 h. Immediately after treatment, cells were harvested and separated into fractions I to IV based on stringency of chromatin association. Equivalent aliquots of each fraction were analyzed by Western blotting for ATM, Mre11, Tax, γH2AX, and H4. (B) Mock-treated (293-CMV) or Tax-transfected (293-Tax) 293 cells were exposed to 10 Gy of gamma irradiation and harvested at 30 min or 1.5 h. Cells were lysed, and extracts were incubated with antibodies against NBS1. Immunoprecipitated (IP) proteins were separated by SDS-PAGE and probed for ATM and NBS1. A Western blot indicating total Tax expression in the transfected 293 cells is shown.

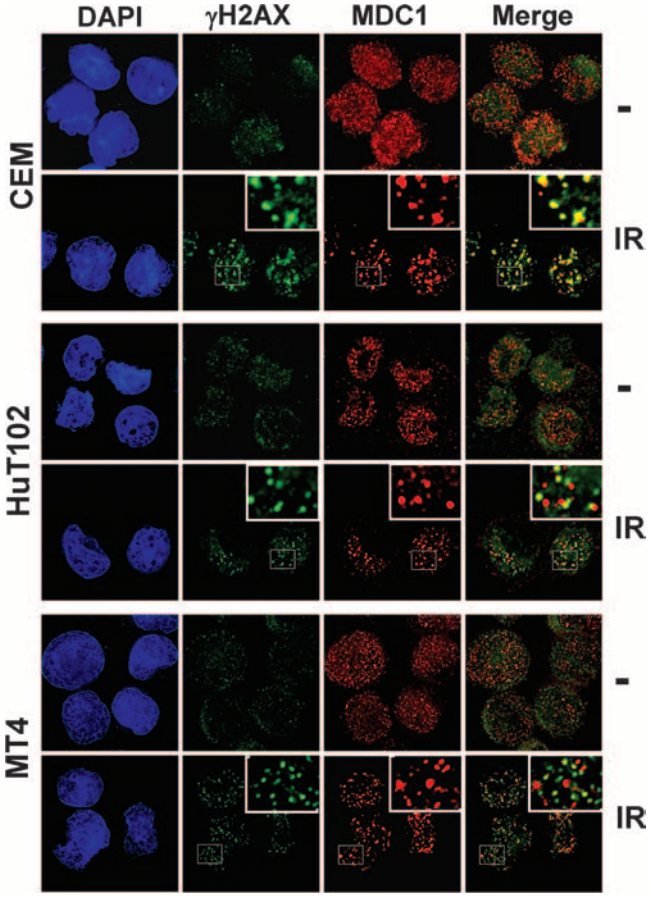

FIG. 8. Tax inhibits the recruitment of MDC1 to DNA repair foci. HTLV-1-negative (CEM) and HTLV-1-infected (HuT102 and MT4) cells were either subjected to mock treatment (−) or exposed to 5 Gy of IR. After 1 h of incubation at 37°C, cells were spun onto coverslips, fixed, and costained with anti-γH2AX (S139) (green) and anti-MDC1 (red) antibodies. A merged image of γH2AX and MDC1 foci is also shown. Images were taken at a magnification of ×100 with an Applied Precision microscope and analyzed with softWoRx image restoration software.

amplification loop, we performed immunofluorescence staining using antibodies against γH2AX and MDC1. In uninfected CEM cells, MDC1 formed nuclear foci that colocalized with γH2AX foci by 1 h after gamma irradiation (Fig. 8). In contrast, MDC1 did not colocalize with γH2AX in HTLV-1-infected HuT102 and MT4 lymphocytes (Fig. 8) after the same dose of irradiation. As noted previously, Tax-expressing cells formed γH2AX foci, albeit less numerous and smaller in size than those seen with control cells. This is consistent with intact initiation of ATM activity in these cells. However, the absence of MDC1 costaining with the DNA damage-induced γH2AX foci suggests that Tax expression interferes with MDC1 binding to Ser139-phosphorylated H2AX. This would inhibit the extension of H2AX phosphorylation over megabases surrounding the DNA break and thus would result in smaller and fewer IR-induced γH2AX foci. Importantly, these findings closely resemble the phenotype of MDC1-deficient cells (31).

By disrupting the binding of MDC1 to γH2AX, Tax interrupts the chromatin-dependent ATM amplification loop, allowing for premature attenuation of the ATM signaling pathway. As a consequence, Tax-expressing cells fail to properly maintain activation of the DNA damage checkpoint and to assemble DNA repair protein complexes, collectively resulting in defective DNA damage repair and premature replication through DNA lesions.

DISCUSSION

To maintain genome stability, cells have regulatory mechanisms that ensure the order and fidelity of cell cycle events, including DNA replication and cell division. These mechanisms become activated upon exposure to genotoxic agents or other adverse conditions such as viral infection. Failure to establish an appropriate DNA damage response results in genomic instability, which is a known causal factor in tumorigenesis. The ATM kinase is a critical transducer of DNA damage signals to checkpoint control and DNA damage repair proteins.

In this report we show that HTLV-1 Tax compromises the ATM-mediated DNA damage response by allowing premature dephosphorylation of ATM and attenuation of ATM kinase activity. Tax does not bind ATM (unpublished data); therefore, we hypothesize that the effect of Tax on ATM dephosphorylation is indirect and may be due to an inability of Tax-expressing cells to amplify and maintain the damage response. Following activation, ATM is initially recruited to DNA breaks where it phosphorylates H2AX, which then serves as a docking site for DNA damage response proteins, including MDC1, 53BP1, and BRCA1. These initial events establish a positive-feedback loop that maintains ATM autophosphorylation and allows the accumulation of active ATM at DSBs. The resulting rapid expansion of H2AX phosphorylation over megabase regions surrounding the break stabilizes the repair locus.

Following IR, Tax-expressing cells show an initial increase in levels of phosphorylated ATM as well as phosphorylation of the ATM substrates NBS1 and Chk2, suggesting that Tax does not affect initial steps in the DNA damage response. However, immunofluorescent staining of phosphorylated ATM revealed an abnormal distribution of smaller, less discrete foci with more diffuse staining in Tax-expressing cells. In addition, ATM was absent from chromatin-rich fractions in bleomycin-treated CREF-Tax cells, whereas a subset of ATM was associated with chromatin in CREF-Neo cells following bleomycin treatment. These results suggest that Tax interferes with the accumulation of ATM on chromatin surrounding DSBs.

Improper accumulation of ATM surrounding DNA breaks compromises the phosphorylation of H2AX over megabases, preventing proper formation of repair foci. Indeed, γH2AX staining following IR was very weak in Tax-expressing cells, with little or no amplification of the γH2AX signal over time. Thus, while phospho-ATM immunostaining increased following DNA damage in the presence of Tax, activated ATM did not accumulate near DSBs, preventing long-range phosphorylation of H2AX and stabilization of the repair foci. Recent studies have reported at least two steps involved in ATM signaling. The initial activation and recruitment of ATM to DNA ends depends on the MRN complex (8, 11, 29, 42, 49), while the subsequent accumulation of ATM on chromatin is regulated by MDC1(31).

MDC1 contains two tandem BRCT domains and an FHA

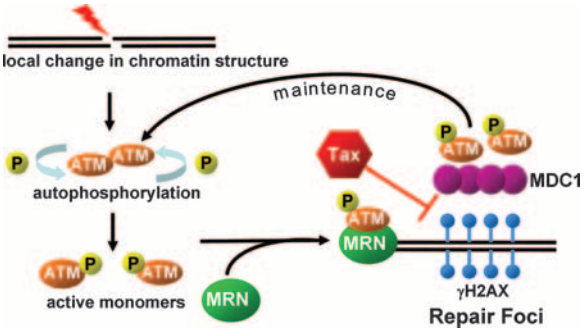

FIG. 9. Model of Tax effects on the ATM-mediated DNA damage response pathway. Tax appears to interfere with the recruitment of MDC1 to DNA repair foci. As a result, p-ATM is not recruited efficiently to these sites and extension of γH2AX is inhibited. The disruption of this positive-feedback signaling results in premature attenuation of the DNA damage response.

domain, which bind to γH2AX and ATM, respectively, and allow it to function as a molecular bridge (31). By binding to γH2AX at the break site, MDC1 helps recruit additional activated ATM molecules, which continue to phosphorylate nucleosomal H2AX away from the break site, creating a positive-feedback loop. The absence of MDC1 from nascent γH2AX foci suggests either that Tax blocks the BRCT domain of MDC1 or, alternatively, that Tax binds to γH2AX, preventing its interaction with MDC1. However, Tax does not appear to alter the cellular amounts of MDC1 or its nuclear localization, as indicated by immunofluorescent staining (Fig. 8). Rather, we hypothesize that Tax interferes with the recruitment of MDC1 to chromatin, preventing stable accumulation of activated ATM into large repair foci and the subsequent amplification of γH2AX. Following DNA damage, Tax may disrupt interactions between ATM, MDC1, and H2AX by competitively interacting with H2AX or MDC1. By interfering with the function of MDC1, which acts as a bridge between ATM and H2AX, Tax appears to disrupt the positive-feedback loop and promote the return of ATM to an unphosphorylated, inactive state (Fig. 9).

Deregulation of cellular phosphatases by Tax may also play a role in ATM inactivation. Tax has been shown to interact with PP2A, a major ATM phosphatase; however, this interaction was reported to inactivate PP2A activity (15), which is not congruent with our findings that Tax promotes ATM dephosphorylation. Recently, we reported that Tax changes cellular localization and protein complex formation in response to cellular stress (18). It is possible that under certain cellular conditions, such as genotoxic stress, Tax alters its interactions with cellular partners, such as phosphatases, resulting in changes in complex formation and function. Defective ATM signaling as observed in Tax-expressing cells would lead to defects in DNA damage checkpoint control.

Tax-expressing cells exhibited a shortened S-phase checkpoint following IR, which is consistent with premature inactivation of ATM kinase activity. Premature inactivation of ATM kinase activity may also affect progression through other phases of the cell cycle. Indeed, a major regulator of the G_2/M checkpoint, Chk2, is activated by ATM phosphorylation. In similarity to ATM activation kinetics results, we found that Chk2 phosphorylation at threonine 68 was robustly induced after DNA damage. However, it was prematurely lost in Tax-expressing cells. Interestingly, Tax has also been shown to bind Chk2 (23, 41). Although the effect of Tax binding on Chk2 kinase activity remains controversial, it has been proposed that Tax might alter the phosphorylation status of Chk2 and prevent its egress from chromatin (22). Thus, Tax appears to regulate Chk2 activity by two different mechanisms: directly by binding to Chk2 and indirectly by modulating ATM kinase activity. Together, these effects influence the DNA damage signaling pathway and have a broad impact on cell cycle progression, apoptosis induction, and DNA repair.

Our results are the first to show that sustained ATM activity, and not just its initial activation, is required to maintain an IR-induced S-phase checkpoint. Premature inactivation of this checkpoint occurs despite the presence of unrepaired DNA in Tax-expressing cells. DNA replication in the presence of unrepaired lesions might increase the accumulation of DNA damage and chromosomal breaks. Indeed, HTLV-1-transformed cells display extensive chromosomal aberrations and Tax expression has been shown to increase gene amplification and mutation frequency (16, 26, 30, 35, 36). Early attenuation of the DNA damage response may be a mechanism by which HTLV-1 controls the cell cycle to gain a proliferative advantage in infected cells. On the other hand, the possibility that virus-mediated regulation of the cell cycle could have a negative impact on the cellular genome is intriguing. Cancer cells are typically characterized by genetic and phenotypic instability, which is referred to as the mutator phenotype. Several researchers have argued that expression of a mutator phenotype is a major factor in tumor progression and that the earliest step in oncogenesis is a change that increases the cellular mutation rate (4). Thus, interference with the ATM-mediated DNA damage response allows Tax to induce a mutator phenotype by decreasing replication fidelity and increasing the mutation rate, which creates a genetically unstable environment susceptible to transformation.

ACKNOWLEDGMENTS

We thank members of the Marriott laboratory for helpful suggestions and editorial comments. We also thank John Brady (National Institutes of Health) for providing anti-Tax antibody 586 and Ron Javier (Baylor College of Medicine) for providing the CREF-Tax and CREF-Neo cell lines.

The study was supported, in part, by U.S. Public Service grant CA-77371 from the National Cancer Institute, National Institutes of Health (awarded to S.J.M.), and grants CA71387 and CA21765 (awarded to M.B.K.) and by the American Lebanese Syrian Associated Charities of the St. Jude Children's Research Hospital. C.C. was supported in part by the National Institutes of Health (training grant AI-07471).

REFERENCES

1. **Andegeko, Y., L. Moyal, L. Mittelman, I. Tsarfaty, Y. Shiloh, and G. Rotman.** 2001. Nuclear retention of ATM at sites of DNA double strand breaks. J. Biol. Chem. **276:**38224–38230.
2. **Bakkenist, C. J., and M. B. Kastan.** 2003. DNA damage activates ATM through intermolecular autophosphorylation and dimer dissociation. Nature **421:**499–506.
3. **Bassing, C. H., K. F. Chua, J. Sekiguchi, H. Suh, S. R. Whitlow, J. C. Fleming, B. C. Monroe, D. N. Ciccone, C. Yan, K. Vlasakova, D. M. Livingston, D. O. Ferguson, R. Scully, and F. W. Alt.** 2002. Increased ionizing radiation sensitivity and genomic instability in the absence of histone H2AX. Proc. Natl. Acad. Sci. USA **99:**8173–8178.
4. **Bielas, J. H., and L. A. Loeb.** 2005. Mutator phenotype in cancer: timing and perspectives. Environ. Mol. Mutagen. **45:**206–213.
5. **Burma, S., B. P. Chen, M. Murphy, A. Kurimasa, and D. J. Chen.** 2001. ATM phosphorylates histone H2AX in response to DNA double-strand breaks. J. Biol. Chem. **276:**42462–42467.

6. **Caron, C., G. Mengus, V. Dubrowskaya, A. Roisin, I. Davidson, and P. Jalinot.** 1997. Human TAF(II)28 interacts with the human T cell leukemia virus type I Tax transactivator and promotes its transcriptional activity. Proc. Natl. Acad. Sci. USA **94:**3662–3667.
7. **Caron, C., R. Rousset, C. Béraud, V. Moncollin, J. M. Egly, and P. Jalinot.** 1993. Functional and biochemical interaction of the HTLV-I Tax1 transactivator with TBP. EMBO J. **12:**4269–4278.
8. **Carson, C. T., R. A. Schwartz, T. H. Stracker, C. E. Lilley, D. V. Lee, and M. D. Weitzman.** 2003. The Mre11 complex is required for ATM activation and the G_2/M checkpoint. EMBO J. **22:**6610–6620.
9. **Celeste, A., S. Petersen, P. J. Romanienko, O. Fernandez-Capetillo, H. T. Chen, O. A. Sedelnikova, B. Reina-San-Martin, V. Coppola, E. Meffre, M. J. Difilippantonio, C. Redon, D. R. Pilch, A. Olaru, M. Eckhaus, R. D. Camerini-Otero, L. Tessarollo, F. Livak, K. Manova, W. M. Bonner, M. C. Nussenzweig, and A. Nussenzweig.** 2002. Genomic instability in mice lacking histone H2AX. Science **296:**922–927.
10. **Chaturvedi, P., W. K. Eng, Y. Zhu, M. R. Mattern, R. Mishra, M. R. Hurle, X. L. Zhang, R. S. Annan, Q. Lu, L. F. Faucette, G. F. Scott, X. T. Li, S. A. Carr, R. K. Johnson, J. D. Winkler, and B. B. S. Zhou.** 1999. Mammalian Chk2 is a downstream effector of the ATM-dependent DNA damage checkpoint pathway. Oncogene **18:**4047–4054.
11. **Difilippantonio, S., A. Celeste, O. Fernandez-Capetillo, H. T. Chen, B. R. San Martin, F. Van Laethem, Y. P. Yang, G. V. Petukhova, M. Eckhaus, L. Feigenbaum, K. Manova, M. Kruhlak, R. D. Camerini-Otero, S. Sharan, M. Nussenzweig, and A. Nussenzweig.** 2005. Role of Nbs1 in the activation of the Atm kinase revealed in humanized mouse models. Nat. Cell Biol. **7:**675–685.
12. **Falck, J., J. Coates, and S. P. Jackson.** 2005. Conserved modes of recruitment of ATM, ATR and DNA-PKcs to sites of DNA damage. Nature **434:**605–611.
13. **Falck, J., N. Mailand, R. G. Syljuasen, J. Bartek, and J. Lukas.** 2001. The ATM-Chk2-Cdc25A checkpoint pathway guards against radioresistant DNA synthesis. Nature **410:**842–847.
14. **Fernandez-Capetillo, O., H. T. Chen, A. Celeste, I. Ward, P. J. Romanienko, J. C. Morales, K. Naka, Z. F. Xia, R. D. Camerini-Otero, N. Motoyama, P. B. Carpenter, W. M. Bonner, J. J. Chen, and A. Nussenzweig.** 2002. DNA damage-induced G_2-M checkpoint activation by histone H2AX and 53BP1. Nat. Cell Biol. **4:**993–997.
15. **Fu, D. X., Y. L. Kuo, B. Y. Liu, K. T. Jeang, and C. Z. Giam.** 2003. Human T-lymphotropic virus type I Tax activates I-kappa B kinase by inhibiting I-kappa B kinase-associated serine/threonine protein phosphatase 2A. J. Biol. Chem. **278:**1487–1493.
16. **Fujita, K., Y. Yamasaki, H. Sawada, Y. Izumi, S. Fukuhara, and H. Uchino.** 1989. Cytogenetic studies on the adult T cell leukemia in Japan. Leuk. Res. **13:**535–543.
17. **Gatei, M., D. Young, K. M. Cerosaletti, A. Desai-Mehta, K. Spring, S. Kozlov, M. F. Lavin, R. A. Gatti, P. Concannon, and K. Khanna.** 2000. ATM-dependent phosphorylation of nibrin in response to radiation exposure. Nat. Genet. **25:**115–119.
18. **Gatza, M. L., and S. J. Marriott.** 2006. Genotoxic stress and cellular stress alter the subcellular distribution of human T-cell leukemia virus type 1 tax through a CRM1-dependent mechanism. J. Virol. **80:**6657–6668.
19. **Goldberg, M., M. Stucki, J. Falck, D. D'Amours, D. Rahman, D. Pappin, J. Bartek, and S. P. Jackson.** 2003. MDC1 is required for the intra-S-phase DNA damage checkpoint. Nature **421:**952–956.
20. **Grassmann, R., M. Aboud, and K. T. Jeang.** 2005. Molecular mechanisms of cellular transformation by HTLV-1 Tax. Oncogene **24:**5976–5985.
21. **Grassmann, R., S. Berchtold, I. Radant, M. Alt, B. Fleckenstein, J. G. Sodroski, W. A. Haseltine, and U. Ramstedt.** 1992. Role of human T-cell leukemia virus type I X region proteins in immortalization of primary human lymphocytes in culture. J. Virol. **66:**4570–4575.
22. **Gupta, S. K., X. Guo, S. S. Durkin, K. F. Fryrear, M. D. Ward, and O. J. Semmes.** 2007. Human T-cell leukemia virus type 1 tax oncoprotein prevents DNA damage-induced chromatin egress of hyperphosphorylated Chk2. J. Biol. Chem. **282:**29431–29440.
23. **Haoudi, A., R. C. Daniels, E. Wong, G. Kupfer, and O. J. Semmes.** 2003. Human T-cell leukemia virus-I tax oncoprotein functionally targets a subnuclear complex involved in cellular DNA damage-response. J. Biol. Chem. **278:**37736–37744.
24. **Jeggo, P. A., and M. Lobrich.** 2006. Contribution of DNA repair and cell cycle checkpoint arrest to the maintenance of genomic stability. DNA Repair **5:**1192–1198.
25. **Jin, D. Y., F. Spencer, and K. T. Jeang.** 1998. Human T cell leukemia virus type 1 oncoprotein tax targets the human mitotic checkpoint protein MAD1. Cell **93:**81–91.
26. **Kamada, N., M. Sakurai, K. Miyamoto, A. Sancar, N. Sadamori, S. Fukuhara, S. Abe, Y. Shiraishi, T. Abe, Y. Kaneko, and M. Shimoyama.** 1992. Chromosome abnormalities in adult T-cell leukemia/lymphoma: a Karyotype Review Committee report. Cancer Res. **52:**1482–1493.
27. **Kao, S. Y., F. J. Lemoine, and S. J. Marriott.** 2001. p53-independent induction of apoptosis by the human T cell leukemia virus type I Tax protein following UV irradiation. Virology **291:**292–298.
28. **Kehn, K., C. L. Fuente, K. Strouss, R. Berro, H. Jiang, J. Brady, R. Mahieux, A. Pumfery, M. E. Bottazzi, and F. Kashanchi.** 2005. The HTLV-I Tax oncoprotein targets the retinoblastoma protein for proteasomal degradation. Oncogene **24:**525–540.
29. **Lee, J. H., and T. T. Paull.** 2005. ATM activation by DNA double-strand breaks through the Mre11-Rad50-Nbs1 complex. Science **308:**551–554.
30. **Lemoine, F. J., and S. J. Marriott.** 2002. Genomic instability driven by the human T-cell leukemia virus type 1 (HTLV-I) oncoprotein, Tax. Oncogene **21:**7230–7234.
31. **Lou, Z., K. Minter-Dykhouse, S. Franco, M. Gostissa, M. A. Rivera, A. Celeste, J. P. Manis, J. van Deursen, A. Nussenzweig, T. T. Paull, F. W. Alt, and J. Chen.** 2006. MDC1 maintains genomic stability by participating in the amplification of ATM-dependent DNA damage signals. Mol. Cell **21:**187–200.
32. **Marriott, S. J., and O. J. Semmes.** 2005. Impact of HTLV-I Tax on cell cycle progression and the cellular DNA damage repair response. Oncogene **24:** 5986–5995.
33. **Mirzoeva, O. K., and J. H. Petrini.** 2003. DNA replication-dependent nuclear dynamics of the Mre11 complex. Mol. Cancer Res. **1:**207–218.
34. **Mirzoeva, O. K., and J. H. J. Petrini.** 2001. DNA damage-dependent nuclear dynamics of the Mre11 complex. Mol. Cell. Biol. **21:**281–288.
35. **Miyake, H., T. Suzuki, H. Hirai, and M. Yoshida.** 1999. Trans-activator Tax of human T-cell leukemia virus type 1 enhances mutation frequency of the cellular genome. Virology **253:**155–161.
36. **Miyamoto, K., N. Tomita, A. Ishii, H. Nonaka, T. Kondo, T. Tanaka, and K. Kitajima.** 1984. Chromosome abnormalities of leukemia cells in adult patients with T-cell leukemia. J. Natl. Cancer Inst. **73:**353–362.
37. **Oakley, G. G., L. I. Loberg, J. Yao, M. A. Risinger, R. L. Yunker, M. Zernik-Kobak, K. K. Khanna, M. F. Lavin, M. P. Carty, and K. Dixon.** 2001. UV-induced hyperphosphorylation of replication protein A depends on DNA replication and expression of ATM protein. Mol. Biol. Cell **12:**1199–1213.
38. **O'Driscoll, M., and P. A. Jeggo.** 2006. The role of double-strand break repair—insights from human genetics. Nat. Rev. Genet. **7:**45–54.
39. **Painter, R. B., and B. R. Young.** 1980. Radiosensitivity in ataxia-telangiectasia: a new explanation. Proc. Natl. Acad. Sci. USA **77:**7315–7317.
40. **Park, H. U., J. H. Jeong, J. H. Chung, and J. N. Brady.** 2004. Human T-cell leukemia virus type 1 Tax interacts with Chk1 and attenuates DNA-damage induced G_2 arrest mediated by Chk1. Oncogene **23:**4966–4974.
41. **Park, H. U., S. J. Jeong, J. H. Jeong, J. H. Chung, and J. N. Brady.** 2005. Human T-cell leukemia virus type 1 Tax attenuates gamma-irradiation-induced apoptosis through physical interaction with Chk2. Oncogene **25:** 438–447.
42. **Paull, T. T., and J. H. Lee.** 2005. The Mre11/Rad50/Nbs1 complex and its role as a DNA double-strand break sensor for ATM. Cell Cycle **4:**737–740.
43. **Rogakou, E. P., C. Boon, C. Redon, and W. M. Bonner.** 1999. Megabase chromatin domains involved in DNA double-strand breaks in vivo. J. Cell Biol. **146:**905–916.
44. **Rogakou, E. P., D. R. Pilch, A. H. Orr, V. S. Ivanova, and W. M. Bonner.** 1998. DNA double-stranded breaks induce histone H2AX phosphorylation on serine 139. J. Biol. Chem. **273:**5858–5868.
45. **Savitsky, K., A. Barshira, S. Gilad, G. Rotman, Y. Ziv, L. Vanagaite, D. A. Tagle, S. Smith, T. Uziel, S. Sfez, M. Ashkenazi, I. Pecker, M. Frydman, R. Harnik, S. R. Patanjali, A. Simmons, G. A. Clines, A. Sartiel, R. A. Gatti, L. Chessa, O. Sanal, M. F. Lavin, N. G. J. Jaspers, A. Malcolm, R. Taylor, C. F. Arlett, T. Miki, S. M. Weissman, M. Lovett, F. S. Collins, and Y. Shiloh.** 1995. A single ataxia-telangiectasia gene with a product similar to Pi-3 kinase. Science **268:**1749–1753.
46. **Sorensen, C. S., R. G. Syljuasen, J. Falck, T. Schroeder, L. Ronnstrand, K. K. Khanna, B. B. Zhou, J. Bartek, and J. Lukas.** 2003. Chk1 regulates the S phase checkpoint by coupling the physiological turnover and ionizing radiation-induced accelerated proteolysis of Cdc25A. Cancer Cell **3:**247–258.
47. **Stewart, G. S., B. Wang, C. R. Bignell, A. M. Taylor, and S. J. Elledge.** 2003. MDC1 is a mediator of the mammalian DNA damage checkpoint. Nature **421:**961–966.
48. **Suzuki, T., S. Kitao, H. Matsushime, and M. Yoshida.** 1996. HTLV-1 Tax protein interacts with cyclin-dependent kinase inhibitor p16 INK4A and counteracts its inhibitory activity towards CDK4. EMBO J. **15:**1607–1614.
49. **Uziel, T., Y. Lerenthal, L. Moyal, Y. Andegeko, L. Mittelman, and Y. Shiloh.** 2003. Requirement of the MRN complex for ATM activation by DNA damage. EMBO J. **22:**5612–5621.
50. **Wang, B., S. Matsuoka, P. B. Carpenter, and S. J. Elledge.** 2002. 53BP1, a mediator of the DNA damage checkpoint. Science **298:**1435–1438.
51. **Xiao, G., E. W. Harhaj, and S. C. Sun.** 2000. Domain-specific interaction with the IκB kinase (IKK) regulatory subunit IKKγ is an essential step in Tax-mediated activation of IKK. J. Biol. Chem. **275:**34060–34067.
52. **Yin, M. J., L. B. Christerson, Y. Yamamoto, Y. T. Kwak, S. Xu, F. Mercurio, M. Barbosa, M. H. Cobb, and R. B. Gaynor.** 1998. HTLV-I Tax protein binds to MEKK1 to stimulate IκB kinase activity and NF-κB activation. Cell **93:**875–884.
53. **You, Z., C. Chahwan, J. Bailis, T. Hunter, and P. Russell.** 2005. ATM activation and its recruitment to damaged DNA require binding to the C terminus of Nbs1. Mol. Cell. Biol. **25:**5363–5379.